

Kinetics Study The Catalyze Mode Of The Formamide Degradation Reaction By Au_x Cluster (X=0, 1, 2, 3): Point, Line Or Surface?



Hongxia Liu* and Zizhong Liu

Chemistry and Environment Science College, China

Received:  October 29, 2018; Published:  November 09, 2018

*Corresponding author: Hongxia Liu, Chemistry and Environment Science College, China

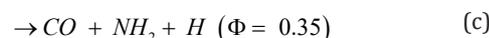
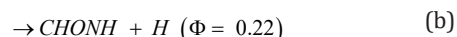
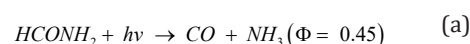
Abstract

The related energy and multi-channel CHONH₂ degradation reaction potential energy surface under the catalysis of Au_x (x=0, 1, 2, 3) cluster was studied, while its dynamic characterization has been investigated with density functional calculations. The geometries were fully optimized with the CCSD(T)//B3PW91 level. We can conclude two results: [1] The calculated results shown that the main pathway of the CHONH₂ degradation reaction under the catalysis of Au_x (x=0, 1, 2, 3) cluster can give the main product P1 (CO+NH₃), while the minor product is P1(H₂+HNCO) and P3 (H₂O+HNC). We calculated the rate constant of the main reaction pathway, the calculated dynamic characterization indicating that the rate constants have the positive temperature dependence. According to the dynamic results and the energetically intermediates and transition states involved in the dominant paths, the reaction is expected to be occurred the most rapidly under the catalysis of Au₂. [2] From the PESs, we can see the present invention, the singlet atom is the best catalysis and can catalyze the reaction better. The present invention studies may provide useful information on the issues of the reaction mechanism and product distributions.

Abbreviations: NBO: Natural Bond Orbital; ED: Electron Density; DFT: Density Functional Theory; PES: Potential Energy Surface; RECP: Relativistic Effective Core Potential; IRC: Intrinsic Reaction Coordinate; SCT: Small Curvature Tunnel Effect Correction

Introduction

Gold has been enjoyed as the most inert metal for a very long time, until the pioneer of Haruta [1,2] found that the gold nanoparticles supported on some metal oxides showed surprisingly high catalytic activity for small molecule reaction at low temperature. , the Nano gold catalysis has picturesque growing in the field of heterogeneous catalysis [3-5]. Technologically, numerous potential industrialization applications of Nano gold catalysts were developed, such as synthesis of fine chemicals [6,7], selective hydrogenations [8,9], water gas shift reaction [10], carbon-carbon bond forming reaction [11], oxidation of organic compounds with molecular O₂ [12,13], pollution and emission control [14] and fuel cell applications [15,16] Scientifically, a huge number of theoretical and experimental studies have been devoted to understand the wide gap between the chemical inertness of bulk gold and high catalytic activity of Nano gold[17-21]. The photolysis of formamide vapor has only been reported [22,23]. They studied the degradation reaction of formamide and gave the three major primary processes:



According to their experimental conditions and results of the quantum yields Φ , the threshold energy of channel a seems to be the lowest. Although the pyrolysis of formamide vapor apparently has not studied previously, several competing channels could also be expected in the thermal system. There are several reports about the competitive reactions in thermal systems [24,25], they conclude that the rate constants increased as the temperature arises. There are still unknown parameters in the descriptions and the rate constants, these two problems have not been entirely settled. Especially for complex bond-breaking reactions, the direct experimental determination of the threshold energy is almost impossible. Ab initio molecular orbital methods have developed rapidly and have provided heats of reaction, potential barriers, molecular geometries, and the vibrational frequencies of several

intermediates and transition states. This valuable information can shed light on reaction mechanisms, and ab initio calculations have been applied to several unimolecular reactions. For complex bond-breaking reactions, information about the transition states is required to test the experimental results.

In the past two decades, the power of computational hardware, software gradually increased and therefore theoretical calculations became more and more popular and important to investigate structures, stabilities and activities of catalysts. calculation relies only on the electron density, which significantly decreases the computational complexities. It becomes an increasingly powerful and useful tool to evaluate various systems, predict catalytic activities, and provide enough accuracy to be compared to experimental data [26]. So far, DFT calculation was widely used to investigate the mechanism of gold catalysis and provide fundamental physical insights into gold catalysis [17,27-28]. For example, self-consistent density functional calculations showing that an isolated Au_{10} cluster should be able to catalyze the CO oxidation reaction even below room temperature and to use calculations can analyze the origin of this effect and suggest that the extraordinary reactivity can be traced back to special reaction geometries available at small particles in combination with an enhanced ability of low coordinated gold atoms to interact with molecules from the surroundings [17,18]. Based on the molecular orbital analysis and the DFT calculations, we have discussed the redistribution of in various bonding and antibonding orbitals and the energy of hyper conjugative interaction stabilization energy ($E(2)$) which have been calculated by natural bond orbital (NBO)[29] analysis using DFT method to give clear evidence of stabilization originating from the hyperconjugation of various intramolecular interactions. The calculations are valuable for providing a reliable insight into the molecular properties.

In this work, we will give a brief review of theoretical investigations on $CHONH_2$ degradation reaction catalyzed by Au_x ($x=0, 1, 2, 3$) cluster, since most of the reviews focused on experimental results and the reviews of theoretical work were relatively rare. No major products are given and there is no available information on product channels, product distributions, and the reaction mechanism in the experiment. Considering the potential importance and the rather limited information, we carry out a detailed theoretical study on the potential energy surface (PES) of the $CHONH_2$ degradation reaction to

- a) Provide the elaborated addition channels on the $CHONH_2$ degradation reaction PESs;

- b) Give a deep insight into the mechanism of $CHONH_2$ degradation reactions;

- c) Calculate the rate constant of the H-abstraction. We hope our work will provide some valuable fundamental insights into title reaction.

Computational Details

All Au clusters and $CHONH_2$ molecule calculations are carried out using the Gaussian 09 program packages [30]. The geometries of all the stationaries are optimized using the hybrid density functional B3PW91 method [31]. As is known, full electron calculations for Au atom consume too much time, so it is necessary to introduce the relativistic effective core potential (RECP) to describe the inner core electrons. The $5s^25p^65d^{10}6s^1$ outermost valence electrons of the Au atom are described through the Lanl2dz base set [32, 33]. In order to obtain more reliable energetic data, higher level single-point energy calculations are performed at the multi-coefficient correlation method based on quadratic configuration interaction with single and double excitations (CCSD(T)) [34-38] by using the B3PW91 optimized geometries. To confirm that the transition states connect designated intermediates or products, intrinsic reaction coordinate (IRC) calculation is carried out at the B3PW91 level. Moreover, the CCSD(T) single-point energies with ZPE corrections are used in the following discussions.

NBO method [39] is performed to study orbital interactions supported by Gaussian 09 program. The localized orbital interactions, involved in non-covalent interactions, are quantified using second order perturbation theory, in which the second-order energy ($E(2)$) was used to measure the interaction strengths. We use the Arrhenius formula to calculate the rate constant. The rate constant of the rate-controlling step along the main reaction channel was calculated among the temperature range 200~2000 K, which considers the small curvature tunnel effect correction (SCT) [40,41].

Results and Discussions

For our convenient discussion, the energy of reactants R is set to be zero for reference. By means of the transition states and their connected isomers or products, a schematic potential energy surface (PES) of the most relevant reaction pathways is described for the $CHONH_2$ degradation reaction catalyzed by Au_x ($x=0, 1, 2, 3$) cluster and the optimized structures of the important stationary points are plotted in (Figure 1).

Table 1: Calculated enthalpies of formation (DH/kcal mol⁻¹) according to eqn (1) for the adsorption $CHONH_2+Au_x$ ($x=0, 1, 2, 3$ and 8) compounds.

A	$CHONH_2+Au_0$	$CHONH_2+Au_1$		$CHONH_2+Au_2$			$CHONH_2+Au_3$		$CHONH_2+Au_8$	
		R1	R2	R1	R2	R3	R1	R2	R1	R2
DH/kcal mol ⁻¹	0	-71.4		-63.5	-43.4		-19.6	-33.2	-33.6	

CHONH₂ Degradation Reaction by Gold Cluster

The Related Energy

Data on formation enthalpies constitute an excellent means to establish whether theoretically predicted phases are likely to be stable, and such data may serve as a guide to evaluate possible reaction routes. For the exploration of the thermodynamic feasibility of accessing these compounds from the elements (eq. (1)) we have also computed the total energies for CHONH₂ + Au_x (x=0, 1, 2, 3) in their ground state structures with full geometry optimization. The adsorption enthalpies for CHONH₂ + Au_x (x=0, 1, 2, 3) were calculated from the difference in the total energy which are summarized in Table 1. The results establish unambiguously that (eq. (1)) expresses endothermic process for CHONH₂ + Au_x (x=0, 1, 2, 3) reaction.

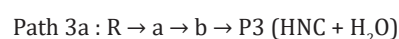
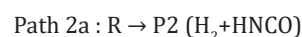
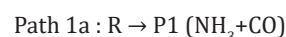


The formation energy for the prototypical CHONH₂+Au₁ are -71.4 and -63.5 kcal/mol respectively, indicating that CHONH₂+Au₁ is a thermodynamically stable phase at ambient conditions. This has already been established by a series of experimental and theoretical studies. Our estimated large positive values for the enthalpy of formation for the CHONH₂+Au₁ series also suggest that it might be possible to degradation compounds by singlet Au catalyzt.

Reaction Potential Energy Surface

A schematic potential energy surface of the CHONH₂ degradation reaction obtained at the CCSD(T)//B3PW91 + ZPE level is plotted in Figure 1a. On the PES for the CHONH₂ degradation reaction, 1,2-hydrogen-abstraction along with the cleavage of C-N bond can give product P1 (NH₃+CO) via the transition state TSRP1. While CHONH₂ also can degradation reaction by other two channels with the barrier TSRP2, TSRa and TSab. In view of the four barriers, it is impossible to overcome the barrier height for these four transition states which the energy barrier is too high. According to the PES in Figure 1a, there are two one-step and one two-steps degradation reaction channels which are the possible reaction pathways. From

the kinetics, the pathway form P3 is more competitive. It needs to overcome the barrier height 71.7 kcal/mol and 40.9 kcal/mol lower than TSRP1 (80.0 kcal/mol) and TSRP2 (93.7 kcal/mol) about 8.3 kcal/mol and 22.0 kcal/mol. Meanwhile, the channel of forming P1 is one-step reaction pathway which is more feasible than two-steps reaction pathway. While from the thermodynamics, the energy of product P1 (5.4 kcal/mol) is lower than P2 and P3 by 10.2 kcal/mol and 25.4 kcal/mol, respectively. Obviously, the formation of P1 is more favorable whatever in kinetics and in thermodynamics. The degradation reaction channel can be described as:



While from the real condition, the most feasible reaction channel is hard to occur and degrade. How to degrade formamide in industrial wastewater has been one of the problems for environmental workers. In this work, we used the Au cluster to catalysis the CHONH₂ degradation reaction. Seen from (Figure 1), and compared to the CHONH₂ degradation reaction, the CHONH₂+Au_x (x=0, 1, 2, 3) reaction mechanism is the same and the formation of P1 is all more favorable whatever in kinetics and in thermodynamics. The energy barrier of the transition state TSRP1 is 80.0 kcal/mol, 31.6 kcal/mol, 23.9 kcal/mol and 55.0 kcal/mol respectively which catalyzed by Au_x (x=0, 1, 2, 3). From a kinetic perspective, the barrier of degradation reaction is the lowest when x=2. On the other hand, from the thermodynamic perspective, the degradation reaction can give off the most heat when x=1. It is shown that the energy variation of the transition state is consistent with the DE variation. However, because the inconsistency between kinetic and thermodynamic conclusions, it is difficult to determine which is the probable value of x in the formamide degradation reaction catalyzed by Au_x (x=0, 1, 2, 3) at different temperature solely based on energies. To provide the exact x value of formamide degradation reaction catalyzed by Au_x (x=0, 1, 2, 3), there is need to perform kinetic calculations.

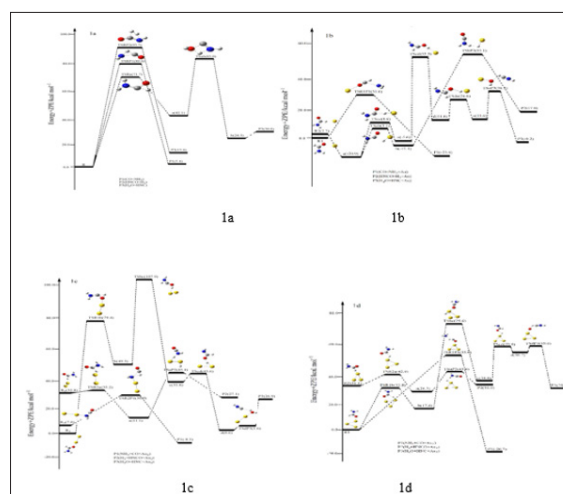


Figure 1: A schematic potential energy surface of the CHONH₂ degradation reaction obtained at the CCSD(T)//B3PW91 + ZPE level.

In summary, starting from Reactant N H₂CHO, we have found three possible reaction channels (Paths 1~3). All the intermediates and transition states of paths (Paths 1~3) proceeding lie above the reactant R at the CCSD(T)//B3PW91 level, therefore, (Paths 1~3) leading to P1 (NH₃+CO), P2 (f + HNCO), and P3 (HNC + H₂O) are much less competitive at normal temperature. Of these three unfeasible paths, we used the Au cluster to catalyze the CHONH₂ degradation reaction. We found Path 1 which forms product P1 (NH₃+CO) is all more favorable whatever in kinetics and in thermodynamics. The relative energy of TSRP1 which catalyzed by Au_x (x=0, 1, 2, and 3) cluster lies 80.0 kcal/mol, 31.6 kcal/mol, 30.9 kcal/mol, and 55.0 kcal/mol; while thermodynamically, the formation of P1 is more favorable by 5.4 kcal/mol, -23.8 kcal/mol, -8.5 kcal/mol, and -20.7 kcal/mol. Thus, we predict that the actual yield of the product P1 may depend on the catalyst in the experiment. Therefore, as reflected in the final product distributions, we predict that (1) a total of three kinds of products P1 (NH₃+CO), P2 (H₂+HNCO), and P3 (HNC + H₂O) should be observed; (2) the major product should be P1 (NH₃+CO), while P2 (H₂+HNCO) and P3 (HNC + H₂O) are the less competitive products; (3) from the thermodynamic perspective, the degradation reaction can give off the most heat when x=1; (4) from a kinetic perspective, the barrier of degradation reaction is the most lowest when the x is equal to 2. Since there is lack of product information in experiment, we hope our present calculation may represent a useful model for understanding the mechanism and provide valuable information for further identification of the product distributions for the title reaction, which is experimentally unknown.

NBO Analysis

The natural bond orbital (NBO) were calculated in order to understand various second-order interactions between the filled orbital of one subsystem and vacant orbital of another subsystem, which is a measure of the intermolecular delocalization or hyperconjugation. NBO analysis provides the most accurate possible "natural Lewis structure" picture of "j" because all orbital details are mathematically chosen to include the highest possible percentage of the electron density. A useful aspect of the NBO method is that it gives information about interactions of both filled and virtual orbital spaces that could enhance the analysis of intra-inter molecular interactions. The second-order Fock-matrix was carried out to evaluate the donor acceptor interactions in the NBO basis. The interactions result in a loss of occupancy from the localized NBO of the idealized Lewis structure into an empty non-Lewis orbital. For each donor (i) and acceptor (j) the stabilization energy (E2) associated with the delocalization i/j is determined as:

$$E(2) = \Delta E_{ij} = q_i \frac{F^2(i, j)}{\epsilon_j - \epsilon_i}$$

where q_i denotes the occupancy of donor orbital, F_(i,j) represents the off-diagonal NBO Fock matrix element and ε_i and ε_j are orbital energies (diagonal elements), respectively. In NBO analysis large E(2) value shows the intensive interaction between electron donors and electron-acceptors and greater the extent of conjugation of the whole system, the possible intensive interactions are given in Table

2. The second-order perturbation theory analysis of Fock matrix in NBO basis shows strong intramolecular hyper-conjugative interactions of p electrons.

Table 2a: Second order perturbation theory analysis of Fock matrix in NBO basis of CHONH₂

Donor(i)	Acceptor (j)	E(2) ^a kJ/mol	E(j)-E(i) ^b (a.u.)	F(i, j) ^c (a.u.)
LP(1) O ₃	BD* C1-H ₂	22.91	0.60	0.106
LP(1) O ₃	BD* C1-N ₄	23.97	0.72	0.119
aLP(1) N ₄	BD* C1-O ₃	60.14	0.29	0.118

^aE(2) means energy of hyper conjugative interaction (stabilization energy).

^bEnergy difference between donor and acceptor i and j NBO orbitals.

^cF(i, j) is the fork matrix element between i and j NBO orbitals.

Table 2b: Second order perturbation theory analysis of Fock matrix in NBO basis of CHONH₂+Au₁.

Donor(i)	Acceptor (j)	E(2) ^a kJ/mol	E(j)-E(i) ^b (a.u.)	F(i, j) ^c (a.u.)
LP(1) O ₃	Lp*c1	86.31	0.16	0.163
LP(1) O ₄	Lp*c1	86.90	0.13	0.150

^aE(2) means energy of hyper conjugative interaction (stabilization energy).

^bEnergy difference between donor and acceptor i and j NBO orbitals.

^cF(i, j) is the fork matrix element between i and j NBO orbitals.

Table 2c: Second order perturbation theory analysis of Fock matrix in NBO basis of CHONH₂+Au₂

Donor(i)	Acceptor (j)	E(2) ^a kJ/mol	E(j)-E(i) ^b (a.u.)	F(i, j) ^c (a.u.)
LP(1) O ₃	BD* C1-N ₂	10.84	0.62	0.107
LP(1) O ₃	BD* C1-N ₄	17.08	0.56	0.126

^aE(2) means energy of hyper conjugative interaction (stabilization energy).

^bEnergy difference between donor and acceptor i and j NBO orbitals.

^cF(i, j) is the fork matrix element between i and j NBO orbitals.

Table 2d: Second order perturbation theory analysis of Fock matrix in NBO basis of CHONH₂+Au₃

Donor(i)	Acceptor (j)	E(2) ^a kJ/mol	E(j)-E(i) ^b (a.u.)	F(i, j) ^c (a.u.)
LP(1)N ₆	BD* C ₄	86.23	0.13	0.148
LP(1) O ₉	BD* C ₄	79.98	0.16	0.160

^aE(2) means energy of hyper conjugative interaction (stabilization energy).

^bEnergy difference between donor and acceptor i and j NBO orbitals.

^cF(i, j) is the fork matrix element between i and j NBO orbitals.

In Table 2, the perturbation energies of significant donor acceptor interactions are present. (1) In CHONH_2 , the interactions between the LP (1) N4 and the anti-bonding of C1-O3 have the highest E(2) value around 60.14 kJ/mol; (2) In $\text{CHONH}_2 + \text{Au}_1$, the interactions between the LP (1) N4 and the anti-bonding of C1 have the highest E(2) value around 86.90 kJ/mol. The other significant interactions giving stronger stabilization energy value of 86.31 kJ/mol to the structure are the interactions between LP (1) O3 and LP* (1) C1; (3) In $\text{CHONH}_2 + \text{Au}_2$, the interactions between the LP (2) O3 and the anti-bonding of C1-N4 have the highest E(2) value around 17.08 kJ/mol; (4) In $\text{CHONH}_2 + \text{Au}_3$, the interactions between the LP (1) N6 and the anti-bonding of C4 have the highest E(2) value around 86.23 kJ/mol. The other significant interactions giving stronger stabilization energy value of 79.98 kJ/mol to the structure are the interactions between LP (3) O9 and LP* (1) C4. Simultaneously, substantial overlaps (Figure 2) of interaction orbitals are reduced along with the decrements of E(2)s. The intermolecular electron transfer occurs from the lone pairs of oxygen atom to the anti-bonding orbitals of C-N bond, which can well explain the breaking of C-N bond easily. Comparing with C-H and N-H bonds et.al, partial orbital interactions between C and N in $\text{CHONH}_2 + \text{Au}_2$ is weaker. Overall, the E(2)s in Table 2 indicates that the C-N bond in $\text{CHONH}_2 + \text{Au}_2$ is weaker than those in $\text{CHONH}_2 + \text{Au}_x$ ($x=0, 1, 3$) to some degree. This result is well consistent with kinetic parameters obtained among reaction Path 1 in above reaction potential energy surface analyses (Figure 3).

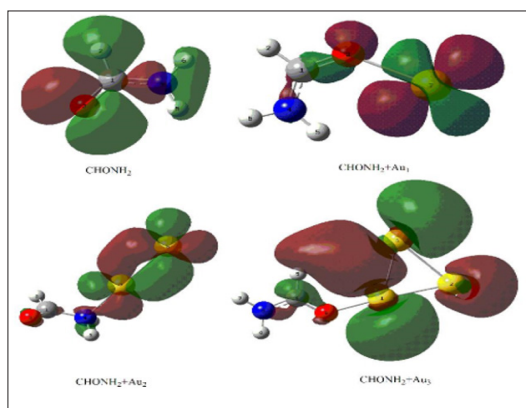


Figure 2: Substantial overlaps of interaction orbitals of the $\text{CHONH}_2 + \text{Au}_x$ ($x=0, 1, 2, 3$) \rightarrow P1 ($\text{NH}_3 + \text{CO} + \text{Au}_x$ ($x=0, 1, 2, 3$))

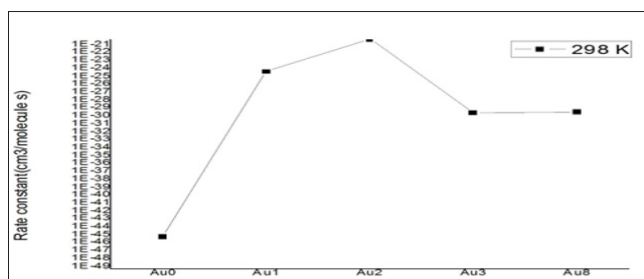


Figure 3: The rate constant of the $\text{CHONH}_2 + \text{Au}_x$ ($x=0, 1, 2, 3$) \rightarrow P1 ($\text{NH}_3 + \text{CO} + \text{Au}_x$ ($x=0, 1, 2, 3$)) at the temperature of 298 K.

Kinetics: In this section, we performed the dynamic calculation for the degradation reaction $\text{CHONH}_2 + \text{Au}_x$ ($x=0, 1, 2, 3$). The calculation of the thermodynamic functions H and S at B3PW91 level was used for obtaining the rate constant results of the dominant channel in the 200~2000 K temperature range. Results are listed in Table 3. Rate constants were calculated as follows:

$$K = (KbT/h) \exp\left(\frac{\Delta_r^\ddagger S_m}{R} - \frac{\Delta_r^\ddagger H_m}{RT}\right)$$

$$A = (KbT/h) \exp\left(\frac{\Delta_r^\ddagger S_m}{R}\right)$$

Where the type of $\Delta_r^\ddagger H_m$ and $\Delta_r^\ddagger S_m$ are respectively for the standard molar activation enthalpy and entropy of reaction system. A is the frequency factor, and kb is Boltzmann constant. It is seen from (Table 3), it shows that the rate constant k of this reaction increases significantly as the temperature increase. Among the range of 200~2000 K, we find that the theoretical rate constants are slightly positive temperature dependence at 200~2000 K. So, it is favorable to the most probable reaction at higher temperature. Seen from Fig.3, compared among these three kinds of reactions, the rate constant of $\text{CHONH}_2 + \text{Au}_2$ is the biggest one which is suitable with the kinetic analysis of the PESs at the temperature of 298 K. Therefore, we hope our present calculation may represent a useful model to understand the mechanism and provide valuable information for the title reaction, and to deeply understand the mechanism of the title reaction.

Table 3a: The thermodynamic functions H and S at B3PW91 level and the rate constants of the $\text{CHONH}_2 \rightarrow \text{P1}$ ($\text{NH}_3 + \text{CO}$) channel in the 200-2000 K temperature range.

T(K)	$\Delta_r^\ddagger S_m$ (J K mol ⁻¹)	$\Delta_r^\ddagger H_m$ (Kj/mol)	$k(s^{-1})$
200	7.594		334.012
298	11.276		334.918
400	13.728		335.766
600	15.803		336.759
800	16.221		337.038
1000	16.037		336.867
1500	14.79		335.281
1700	14.209		334.351

Table 3b: The thermodynamic functions H and S at B3PW91 level and the rate constants of the $\text{CHONH}_2 + \text{Au}_1 \rightarrow \text{P1}$ ($\text{NH}_3 + \text{CO} + \text{Au}_1$) channel in the 200-2000 K temperature range.

T(K)	$\Delta_r^\ddagger S_m$ (J K mol ⁻¹)	$\Delta_r^\ddagger H_m$ (Kj/mol)	$k(s^{-1})$
200	54.982	229.287	4.0×10^{-45}
298	63.731	231.433	4.7×10^{-25}
400	69.166	233.305	1.2×10^{-14}
600	73.781	235.52	2.8×10^{-4}
800	74.915	236.279	5.1×10^1
1000	74.843	236.205	7.8×10^4
1500	73.366	234.324	1.5×10^9
1700	72.68	233.232	1.5×10^{10}
1900	72.007	232.026	9.5×10^{10}

Table 3c: The thermodynamic functions H and S at B3PW91 level and the rate constants of the $\text{CHONH}_2 + \text{Au}_2 \rightarrow \text{P1} (\text{NH}_3 + \text{CO} + \text{Au}_2)$ channel in the 200-2000 K temperature range.

T(K)	$\Delta_r^{\ddagger}S_m$ (J K mol ⁻¹)	$\Delta_r^{\ddagger}H_m$ (KJ/mol)	$k(s^{-1})$
200	21.853	195.979	3.8×10^{-38}
298	26.016	197.003	4.2×10^{-21}
400	28.769	197.951	3.7×10^{-12}
600	30.92	198.976	2.4×10^{-3}
800	31.041	199.036	7.0×10^1
1000	30.455	198.503	3.5×10^4
1500	28.38	195.903	1.4×10^8
1700	27.568	194.608	1.0×10^9
1900	26.803	193.231	4.8×10^9
2000	26.439	192.525	9.4×10^9

Table 3d: The thermodynamic functions H and S at B3PW91 level and the rate constants of the $\text{CHONH}_2 + \text{Au}_3 \rightarrow \text{P1} (\text{NH}_3 + \text{CO} + \text{Au}_3)$ channel in the 200-2000 K temperature range.

T(K)	$\Delta_r^{\ddagger}S_m$ (J K mol ⁻¹)	$\Delta_r^{\ddagger}H_m$ (KJ/mol)	$k(s^{-1})$
200	57.245	259.866	5.5×10^{-53}
298	67.086	262.274	2.1×10^{-30}
400	72.919	264.283	1.6×10^{-18}
600	77.898	266.679	8.9×10^{-7}
800	79.354	267.664	7.8×10^{-1}
1000	79.575	267.853	3.0×10^3
1500	78.613	266.6	2.1×10^8
1700	78.057	265.718	2.9×10^9
1900	77.496	264.704	2.3×10^{10}
2000	77.212	264.155	5.7×10^{10}

Conclusion

We have presented a detailed investigation on the related energy and multi-channel CHONH_2 degradation reaction potential energy surface under the catalysis of Au_x ($x=0, 1, 2, 3$) cluster and its dynamic characterization using a detailed quantum chemical methods. The following important conclusions are obtained

- The prediction of CHONH_2 degradation reaction under the catalysis of Au_x ($x=0, 1, 2, 3$) cluster with large positive formation enthalpy hopefully will inspire and guide catalysis efforts in this direction. NBO theory is applied to characterize the nature of the intermolecular orbital interactions in the $\text{CHONH}_2 + \text{Au}_x$ ($x=0, 1, 2, 3$). The calculation show that the maximum formation energy and thermodynamics prove that the $\text{CHONH}_2 + \text{Au}_1$ reaction is the most possible, while kinetic and NBO analyses prove that reaction $\text{CHONH}_2 + \text{Au}_2$ is the most plausible. In summary, the rate constant of $\text{CHONH}_2 + \text{Au}_2$ is the biggest one which is suitable with the kinetic and NBO analysis.
- The multi-channel CHONH_2 degradation reaction potential energy surface under the catalysis of Au_x ($x=0, 1, 2, 3$) cluster is performed to explore the reaction mechanism. Our calculation show that one primary channel is obtained which the H-shift

reaction can give the main product P1 ($\text{NH}_3 + \text{CO} + \text{Au}_x$ ($x=0, 1, 2, 3$)). And $\text{CHONH}_2 + \text{Au}_x$ ($x=0, 1, 2, 3$) reaction occurs mainly in the high-temperature range which plays a more important role as the temperature increase. The present theoretical studies may provide useful information on the reaction mechanism.

c) The dynamic characterization show that the theoretical rate constants are slightly positive temperature dependence at 200~2000 K. The rate constant k of this reaction increases significantly as the temperature increase. The analyses consistently support the notion that the formamide degradation reaction can be catalyzed by singlet atom whatever point, line and surface in catalysts. Until now, there are no experimental studies available to verify our results, but we hope to motivate experimentalists to measure the rate constant.

Acknowledgement

The project was supported by the Higher educational Scientific research projects of Inner Mongolia (NJZY030), the Natural Science Foundation of Inner Mongolia (2012MS0218), the Talent Development Foundation of Inner Mongolia, the Inner Mongolia Normal University Research Fund Project (KYZR1119, 2017ZRZD001), the Natural Science Foundation of Inner Mongolia (2014BS0206), and the Scientific research project of the Inner Mongolia colleges and Universities (NJZY030).

References

- Haruta M, Kobayashi T, Sano H, Yamada N (1987) Novel gold catalysts for the oxidation of carbon monoxide at a temperature far below 0°C. Chem Lett 16: 405-408.
- Okumura M, Fujitani T, Huang JH, Ishida TA (2015) Career in catalysis: masa take haruta ACS Catal. 5: 4699-4707.
- Takei T, Akita T, Nakamura I, Fujitani T (2012) Chapter one heterogeneous catalysis by gold Adv Catal. 55: 1-126.
- Okumura M, Haruta M (2016) Interplay of theoretical calculations and experiments for a study of catalysis by gold Catal Today. 259(50): 81-86.
- Huang JH, Akita T, Faye J, Fujitani T, Takei T, et al. (2009) Propene epoxidation with dioxygen catalyzed by gold clusters. Angew Chem Int Ed 48: 7862-7866.
- Hashmi ASK, Hutchings G (2006) Gold catalysis. J Chem Int Ed, 45: 7896-7936.
- Huang JH, Takei T, Ohashi H, Haruta M (2012) Propene epoxidation with oxygen over gold clusters: Role of basic salts and hydroxides of alkalis. Appl Catal A 435: 115-122.
- Bailie JE, Hutchings GJ (1999) Promotion by sulfur of gold catalysts for crotyl alcohol formation from crotonaldehyde hydrogenation Chem Commun. 2151-2152.
- Corma A, Serna P (2006) Chemo selective hydrogenation of nitro compounds with supported gold catalysts Science. 313(5785): 332-334.
- Fu Q, Saltsburg H, Flytzani Stephanopoulos M (2003) Active nonmetallic Au and Pt species on ceria-based water gas shift catalyst. Science 301(5635): 935-938.
- Carrettin S, Guzman J, Corma A (2005) Supported gold catalyzes the homocoupling of phenylboronic acid with high conversion and selectivity. Angew Chem Int Ed 44: 2242-2245.
- Hughes MD, Xu YJ, Jenkins P, McMorn P, Landon P, et al. (2005) Tunable gold catalysts for selective hydrocarbon oxidation under mild conditions. Nature 437: 1132-1135.

13. Huang JH, Haruta M (2012) Gas phase propene epoxidation over coinage metal catalysts. *Res Chem Inter med* 38(1): 1-24.
14. Patrick G van der Lingen E, Corti CW, Holliday RJ, Thompson DT (2004) The potential for use of gold in automotive pollution control technologies: a short review *Top Catal.* 30-31: 273-279.
15. Corti CW, Holliday RJ, Thompson DT (2005) Commercial aspects of gold catalysis. *Appl Catal A* 291: 253-261.
16. Peplow M (2013) The accelerator. *Nature* 495(7440): S10-S11.
17. Liu ZP, Gong X, Kohanoff QJ, Sanchez C, Hu P (2003) Catalytic role of metal oxides in gold-based catalytic: a first principles study of CO oxidation on TiO₂ supported Au. *Phy Rev Lett* 91: 1-4.
18. Lopez N, Norskov JK (2002) Catalytic CO oxidation by a gold nanoparticle: a density functional study. *J Am Chem Soc* 124: 11262-11263.
19. Iizuka Y, Tode T, Takao T, Yats K, Takeuchi T, Tsubota S (1999) A kinetic and adsorption study of CO oxidation over unsupported fine gold powder and over gold supported on Titanium dioxide. *J Catal* 187: 50-58.
20. Maeda Y, Iizuka Y, Kohyama M (2013) Generation of oxygen vacancies at an Au/TiO₂ perimeter interface during CO oxidation detected by in situ electrical conductance measurement. *J A Chem Soc* 135: 906-909.
21. Uchiyama T, Yoshida H, Kuwauchi Y, Ichikawa S, Shimada S (2011) Systematic morphology changes of gold nanoparticles supported on CeO₂ during CO oxidation. *Angew Chem Int Ed* 50: 10157-10160.
22. Boden JC, Back RA (1970) Photochemistry and free-radical reactions in formamide vapor. *Trans Faraday Soc* 66: 175-182.
23. Kskumoto T, Saito KO, Imamura A (1985) Thermal decomposition of formamide: shock tube experiments and ab initio calculations. *J Phys Chem* 89(11): 2286-2291.
24. Klein IE, Rabinovitch BS, Jung KH (1977) Vibrational energy transfer by a competitive channel method in thermal unimolecular systems. A definitive measurement of the temperature dependence of collisional efficiency. *J Chem Phys* 67: 3833-3835.
25. Just T, Troe J (1980) Theory of Two-Channel Thermal Unimolecular Reactions. 1 General Formulation *J Phys Chem* 84(23): 3068-3072.
26. Lee SS, Fan CY, Wu TP, Anderson SL (2004) CO oxidation on Au_n/TiO₂ catalysts produced by size-selected cluster deposition. *J Am Chem Soc* 126: 5682-5683.
27. Molina LM, Hammer B (2003) Active role of oxide support during CO oxidation at Au/MgO. *Phys Rev Lett* 90(20): 1-4.
28. Sun KJ, Kohyama M, Tanaka S, Takeda S (2015) Understanding of the activity difference between nanogold and bulk gold by relativistic effects. *J Energ Chem* 24(4): 485-489.
29. Hou XF, Yan LL, Huang T, Hong Y, Miao SK, Peng XQ (2016) A density functional theory study on structures, stabilities, and electronic and magnetic properties of Au_nC (n=1-9) clusters. *Chem Phys* 472(15): 50-60.
30. Frisch GW, Trucks HB, Schlegel GE, Scuseria MA, Robb JR (2010) Gaussian 09, revision D 01 Wallingford CT: Gaussian Inc.
31. Truhlar DG, Garrett BC, Klippenstein S (1996) Current status of transition-state theory. *J Phys Chem* 100: 12771-12800.
32. Hay PJ, Wad WR (1985) Ab initio effective core potentials for molecular calculations. Potentials for the transition metal atoms Sc to Hg. *J Chem Phys* 82: 270-283.
33. Hay PJ, Wad, WR (1985) Ab initio effective core potentials for molecular calculations. Potentials for K to Au including the outermost core orbitals. *J Chem Phys* 82: 299-310.
34. Scuseria GE, Schaefer HF (1989) Is coupled cluster singles and doubles (CCSD) more computationally intensive than quadratic configuration interaction (QCISD)? *J Chem Phys* 90: 3700-3703.
35. Dunning Jr TH (1989) Gaussian basis sets for use in correlated molecular calculations. The atoms boron through neon and hydrogen. *J Chem Phys* 90: 1007-1023.
36. Kendall RA, Dunning Jr TH (1992) Electron-affinities of the 1st-row atoms revisited-systematic basis-sets and wave-functions. *J Chem Phys* 96: 6796-6806.
37. Woo, DE, Dunning Jr (1993) Gaussian basis sets for use in correlated molecular calculations. III. The atoms aluminum through argon. *J Chem Phys* 98: 1358-1371.
38. Wilson AK, Woon DE, Peterson KA, Dunning Jr TH (1999) Gaussian basis sets for use in correlated molecular calculations: IX The atoms gallium through krypton. *J Chem Phys* 110: 7667-7676.
39. Glendening ED, Landis CR, Weinhold F (2012) Natural bond orbital methods. *WIREs Comput Mol Sci* 2: 1-42.
40. Lu DH, Truong TN, Melissas VS, Lynch, GC, Liu YP (1992) Polyrate 4:a new version of a computer program for the calculation of chemical reaction rates for polyatomics. *Comput Phy Commun* 71(3): 235-262.
41. Liu YP, Lynch GC, Truong TN, Lu DH, Truhlar DG et al. (1993) Molecular modeling of the kinetic isotope effect for the [1,5] sigma tropic rearrangement of cis-1,3-pentadiene. *J Am Chem Soc* 115: 2408-2415.

ISSN: 2574-1241

DOI: 10.26717/BJSTR.2018.10.002024

Hongxia Liu. Biomed J Sci & Tech Res



This work is licensed under Creative Commons Attribution 4.0 License

Submission Link: <https://biomedres.us/submit-manuscript.php>

Assets of Publishing with us

- Global archiving of articles
- Immediate, unrestricted online access
- Rigorous Peer Review Process
- Authors Retain Copyrights
- Unique DOI for all articles

<https://biomedres.us/>